

# A Simple Voltage-Modulated Markov Chain Model for the Piezo1 Ion Channel to Investigate Electromechanical Pacing

Dennis Ogiermann<sup>1</sup>, Abdulaziz Mohamed<sup>1</sup>, Luigi E. Perotti<sup>2\*</sup>, Daniel Balzani<sup>1</sup>

<sup>1</sup>Chair of Continuum Mechanics, Ruhr-Universität Bochum,  
Universitätsstraße 150, 44801 Bochum, Germany

<sup>2</sup>Department of Mechanical and Aerospace Engineering, University of Central Florida  
Orlando, USA

\*E-mail address of corresponding author: Luigi.Perotti@ucf.edu

**Abstract** Piezo1 ion channels are stretch-activated ion channels involved in a variety of important physiological and pathophysiological processes, as for example cardiovascular development and homeostasis. Since its discovery, it is known that this type of ion channel desensitize when exposed to stretch. However, recent experiments on Piezo1 ion channels have uncovered that their stretch response is qualitatively different when exposed to positive electrochemical driving forces, where the desensitization is reset. In this work, we propose a novel voltage-modulated mathematical model of Piezo1 based on a continuous-time Markov chain. We show that our Piezo1 model is able to quantitatively reproduce a wide range of experimental observations. Furthermore, we integrate our new ion channel model into the Mahajan-Shiferaw ventricular cardiomyocyte model to study the effect of electromechanical pacing at the cellular scale. This integrated cell model is able to qualitatively reproduce some aspects of the experimental observations regarding the rate-dependence of electromechanical pacing protocols. Our studies suggest that the Piezo1 ion channel is an important component that significantly contributes to the electromechanical coupled response of cardiomyocytes.

**Keywords:** Stretch-activated ion channel, Mechanosensitive ion channel, Mechano-electric feedback, Mechano-chemical feedback, Cardiac electromechanics

## 1 Introduction

The computational analysis of physiological and patho-physiological heart function has been of increasing interest due to the large potential for improving medical intervention as well as enhancing the fundamental understanding of the underlying processes [53, 9, 54, 16, 50, 60, 26, 1, 47, 8, 45, 48]. Especially the electromechanical coupling has attracted particular interest since it dominates the active contraction behavior [24, 22, 21, 2, 19]. Interestingly, the mechano-electric feedback has been given less attention, although it is important for many processes in the heart which can be linked to clinically relevant questions. For instance, this back-coupling of mechanics onto the chemical processes governs adaptive processes, including patho-physiological growth and homeostasis [42, 3]. Another example is Cardiopulmonary resuscitation (CPR), a standard emergency procedure [49, 52] in which fast and deep chest compressions are applied in subjects suffering cardiac arrest to maintain a minimal level of blood circulation until more advanced care can be administered. Here, optimized procedure protocols may be identified by additionally exploiting the active contraction response of the heart that may be triggered mechanically. Furthermore, existing medical procedures also

exploit this back-coupling. For instance, approaches such as precordial thump [51] and percussion pacing [62] aim at conditioning heart pacing using mechanical stimuli. The European Resuscitation Society (ERS) recommends that percussion pacing can be attempted during bradycardia, if no pacing equipment is available and atropine treatment is ineffective [52]. Unfortunately, precordial thump and percussion pacing have not yet been sufficiently investigated and the American Heart Association (AHA) recommends against using these procedures in a general clinical setting since existing clinical studies on these techniques do not show strong evidence of being effective or ineffective [49]. Here, computational analysis may supply the necessary insight, provided that suitable models for an accurate description of the back-coupling are available. Interestingly, despite the importance of emergency pacing techniques, no theoretical framework exists to understand its mechanisms in detail.

Understanding the mechanism linking pacing and mechanical stimuli is certainly difficult and there have not been many experimental studies in this area [29]. In this context, Quinn and Kohl [55] investigated a rabbit heart subjected to several sequences of mechanical and electrical stimuli during sinus rhythm. The rabbit heart is in Langendorff perfusion with an inserted intraventricular balloon to simulate blood pressure. During the application of mechanical and electrical stimuli to the ventricular epicardium, the balloon pressure and transmembrane voltage at a point on the ventricular epicardium are recorded. In these experiments, several key features are identified: 1) There is a reversible, frequency-dependent loss of capture of mechanical pacing that depends on the number of applied mechanical stimuli; 2) Alternating the application of mechanical and electrical stimuli leads to a faster loss of capture (in the number of applied mechanical stimuli) than when only mechanical pacing is applied. The coupling between mechanical and electrical pacing found in these experiments cannot be explained by current models and highlights the importance of developing a theoretical framework for mechanical pacing of cardiac tissue.

Stretch-activated ion channels modulate ionic balances in cells including cardiomyocytes. In this paper, we assume that PIEZO channels are a major contributor to this mechanism. The PIEZO protein family consists of mechanically activated cation-selective channels [14, 33], which govern a wide range of physiological functions across several animal kingdoms [13]. Vertebrates express primarily the isoforms Piezo1 and Piezo2 [13], which can be functionally identified as biological sensors for mechanical stimuli [34]. The characteristic feature of PIEZO ion channels is a significantly voltage-dependent [44] slow (Piezo1) and fast (Piezo2) inactivation kinetics [64], which has been demonstrated to allow a frequency-dependent response to periodic mechanical stimuli. Recent research has uncovered that this class of ion channels is involved in many physiological and pathophysiological processes. In tactile neurons, Piezo2 plays a key role in the touch sensation of rough surfaces [34]. Experiments also suggest that PIEZO channels act as pressure overload sensors in ventricular cardiomyocytes [3, 66] with implications in cardiovascular development [58, 35] and homeostasis [35, 3, 6, 37, 66, 65, 7]. In addition, experiments have been able to link Piezo1 upregulation to pathophysiological processes such as hypertrophy [71, 3, 30], arrhythmia [30], and heart failure [36, 30]. Although it has been shown that PIEZO ion channels are expressed in the ventricular myocardium [36], it has only been recently demonstrated that Piezo1 channels are located in the transverse tubular system of cardiomyocytes [30, 66]. Interestingly Piezo1 and Piezo2 are involved in physiological processes outside the neural and cardiovascular systems, as mutations have been linked to severe diseases, e.g., hereditary xerocytosis [68, 4], Marden-Walker syndrome, and Gordon syndrome [43] in humans.

In this work, we will analyze a simplified version of the experiment by Quinn and Kohl [55] via mathematical modeling and simulation studies. As a first step, we will motivate why we believe that these experimental observations are related to Piezo1 ion channels. Subsequently, we will

develop a Piezo1 voltage-modulated, continuous-time Markov chain model on the basis of the experiments in [34, 33] and Moroni et al. [44]. This ion channel model will then be integrated in the well-known rabbit ventricular cardiomyocyte model by Mahajan et al. [41] to investigate the qualitative role of Piezo1 [13] channels during mechanical and electromechanical pacing of the cardiac tissue. Finally, we will discuss the model limitations and several possibilities to improve and refine the model in subsequent studies.

## 2 Methods

### 2.1 Model Construction

In this section we construct a mathematical model of a rabbit ventricular cardiomyocyte, which is capable of explaining, at least qualitatively, the experimental observations in Quinn and Kohl [55]. In these experiments, the authors applied electrical and mechanical stimuli to Langendorff-perfused rabbit hearts while measuring their electrical response. Mechanical stimuli have been applied using a piston against the left ventricular (epicardial) wall, while electrical stimuli have been applied using an electrode to deliver local currents to the left ventricle epicardium. Both mechanical and electrical stimulation sites have been chosen to be spatially close. Another electrode on the left ventricular wall (epicardial) has measured the electrical activity. The main observation is that, at first, the ventricle responds to the mechanical stimuli with a full depolarization, which we call *mechanical capture*. After a few mechanical stimuli (see, e.g., fig. 3A), the ventricle stops responding, which is called *loss of (mechanical) capture*. The exact number of mechanical stimuli until loss of capture depends on the stimulus frequency and the number of applied electrical stimuli in-between two mechanical stimuli. The observed loss of capture is reversible, and mechanical capture is restored after mechanical stimuli have not been applied for a sufficiently long time window [55, 44].

#### 2.1.1 Determination of the Molecular Candidate for the Ion Channel Model

The ion channels to be included in the model need to generate enough current to depolarize the membrane after sufficient deformation. Generally, the currents generated by the deformation of cells are categorized into two broad classes: non-selective stretch-activated ion channels  $I_{\text{SAC,NS}}$  and  $\text{K}^+$ , and selective stretch-activated ion channels  $I_{\text{SAC,K}}$ . For healthy cardiomyocytes in a physiological environment it can be shown that, assuming an Ohmic current generated by the flux of ions through an ion channel, the reversal potential of  $\text{K}^+$  ( $\approx -90 \text{ mV}$ ) is below the depolarization threshold ( $\approx -60 \text{ mV}$ ). Hence, activating these ion channels cannot induce membrane depolarization. We refer to e.g. [56] for more details. This narrows down the candidates for the ion channels. Only the PIEZO family and the TRP family of ion channels are known to be primary generators of  $I_{\text{SAC,NS}}$  [59].

Obviously, the candidate ion channels also have to be expressed in real cardiomyocytes. In addition, we assume that the ion channel is located on the cell membrane to depolarize, since this location may be more responsive to mechanical deformation. Although we acknowledge the possibility that the hypothetical ion channel can be located inside the sarcoplasmic reticulum, we do not follow this idea in the first iteration of the integrated model proposed here. This choice restricts the possible ion channel candidates, as some TRP channels are not located on the cell membrane (see e.g., [67] for an overview). For the PIEZO family, it has been shown in experimental studies that both channels expressed in vertebrates are localized near the transverse tubular system of cardiomyocytes [30, 32]. Note that additional experiments suggest the existence of a protective mechanism downregulating PIEZO channels' activity when these channels are integrated into the endoplasmic membrane [69]. These experiments provide further evidence that the Piezo1 channels responsible, at least in large

part, for the cardiomyocyte electromechanically coupled response (the focus of the current work) is on the sarcoplasmic membrane.

Finally, based on the experimental observation, we hypothesize that the ion channel needs to feature slow frequency-dependent inactivation. This rules out that TRP channels alone will be responsible for the behavior observed in the mechanical pacing experiments by [55] and leaves the PIEZO family as an optimal candidate as the experiments of [34] provide strong evidence for their frequency-dependent behavior. The PIEZO family has two known members, Piezo1 and Piezo2. The latter features fast inactivation (see, e.g., [34]), which further narrows down our choice to the Piezo1 channel.

More evidence against the TRP channels being the primary candidate to explain the experimental observation in [55] is provided by recent studies. Experiments by Nikolaev et al. [46] suggest that most TRP channels might not be inherently stretch-activated. Instead, they hypothesize that TRP channels play a role downstream in mechanosensation pathways. This hypothesis is further supported by more recent experiments on the interplay between TRPM4 and Piezo1, showing colocalization of these ion channels in the transverse-axial tubular system of ventricular cardiomyocytes in different species [30, 66].

**2.1.2 Improved Piezo1 Continuous-Time Markov Chain Model** Three distinct mathematical models for Piezo1 have been proposed in the literature. Bae et al. [5] have proposed a continuous-time Markov chain model with three states (open, closed, and inactivated), which are fully connected and which feature a pressure-dependent transition from the closed to the open state and from the inactivated to the closed state. This is an extension of a linear Markov chain where the closed and inactivated states are disconnected, see [25]. This model has been shown to capture well the fast inactivation behavior in response to single mechanical stimuli. Modal analysis of a coarse-grained Piezo1 model [72] further supports the model assumption that there are indeed at least three independent states.

Lewis et al. [34] have proposed a similar model. Based on the argument that the inactivation kinetics of PIEZO ion channels in two-step pressure stimulation protocols can be fitted well with two exponentials, Lewis et al. [34] hypothesized that there are two distinct inactivation states. They corroborated this hypothesis by showing that the three state models [25, 5] fail to explain a new set of experiments on frequency-dependent stimulus response of mouse Piezo1 and Piezo2 channels. Therein Piezo1 has been shown to act as a band-pass filter on sinusoidal pressure stimuli. Their proposed model contains four states, containing the same cycle as Bae et al. [5]’s model and an additional second inactivation state with constant rates, which has been bidirectionally connected to the open state. Lewis et al. [34] showed that this model can capture well the frequency-dependent behavior of Piezo1 and Piezo2 ion channels. Although we were able to identify a recent experimental investigation of the mechanism of inactivation by Zheng et al. [73] supporting the hypothesis of the existence of two possibly distinct inactivation states for the Piezo1 channel, further studies are required to determine whether these states are coupled or truly distinct. In addition, the model from Lewis et al. [34] lacks the voltage-dependent behavior seen in other experiments (e.g., [64, 44]).

Finally, there is the recent Hodgkin-Huxley formulation by Zhang and Zou [70] with three independent gates featuring both voltage-modulation and stretch activation, which distinguishes it from the previous models. A possible drawback of this model is that existing simulations on the molecular dynamics of Piezo1 [72, 15, 11] and structural investigations of it [61] suggest a global transition structure between independent energy states of the ion channel, as reflected in the previously published Markov chain models discussed in the paragraphs above. Furthermore, experiments on the electrophysiological properties of Piezo1 suggest a voltage-dependence between inactivation and activation [64, 44]. This violates the assumption

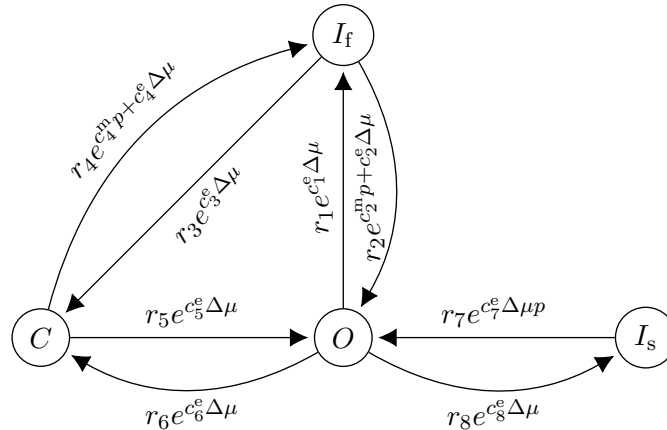


**Figure 1:** Continuous-time Markov chain of the proposed Piezo1 model extending the model of [34]. Analogously to the original work, the proposed model contains an open state  $O$ , fast and slow inactivation states  $I_f$  and  $I_s$ , and a closed state  $C$ .  $p$  denotes the pressure, and  $\Delta\mu$  the electrochemical driving force acting on the channel. Since the reversal potential of PIEZO channels is hypothesized to be approximately 0 (i.e.  $E_r = 0$ ), we obtain  $\Delta\mu = \varphi_m - E_r = \varphi_m$ , where  $\varphi_m$  denotes the transmembrane potential. Exponential transition functions have been chosen in conformance to Eyring’s classical transition state theory [18, 17]. The parameters are grouped into rate coefficients  $r_i$ , mechanical pressure coefficients  $c_i^m$  and electrochemical driving force coefficients  $c_i^e$ . We want to highlight that the transition rate between the slow inactivating state  $I_s$  and the open state  $O$  is made dependent on the product of the electrochemical driving force and the pressure.

of Hodgkin-Huxley models that the ion channel opens via independently acting gates. The authors provide different sets of parameters per experiment and per applied stimulus in each experiment, resulting in no continuous dependence of the gating variables on the pressure, underlining this problem. While this does not exclude the existence of a Hodgkin-Huxley type model, a different approach may avoid the outlined issue and therefore we will not consider Hodgkin-Huxley type models for the Piezo1 channel in this work.

With the information gathered from these previous models we constructed a 4 state Markov chain shown in figure 1. We started the model construction with the Markov chain described by Lewis et al. [34]<sup>1</sup>. To introduce the voltage-modulation into the model, we added a linear voltage term in each exponent and the resulting model retained, at least in principle, the frequency-dependent behavior described in Lewis et al. [34]. A description of the parameter optimization procedure can be found in Section 2.2. Based on this procedure, we were unable to eliminate any of the voltage terms introduced in the model (through regularization with  $\gamma > 0$ , cf. eq. 6). For the model construction procedure, we have utilized *Catalyst.jl* [39] and *ModelingToolkit.jl* [40]. The model is also provided as supplementary material via *CellML 2.0* [12], where it has been validated via *OpenCOR* [20].

**2.1.3 Ventricular Cardiomyocyte Model** Our main goal is to derive a cell model able to describe as many mechanical pacing experiments by Quinn and Kohl [55] as possible. These experiments were conducted on rabbit hearts at high pacing rates, and thus we decided to utilize the Mahajan-Shiferaw ventricular cardiomyocyte model [41] as our foundation. Indeed, the Mahajan-Shiferaw model was constructed for exactly this type of scenarios. We have

<sup>1</sup>We explored many different formulations, from linear to more complex topologies with multiple cycles. However, we decided to present this topology, since it is connected to other numerical experiments, as a similar model has been used in previous computational studies of Piezo1, and since it yielded sufficiently good fits to the data with a comparably low number of parameters.

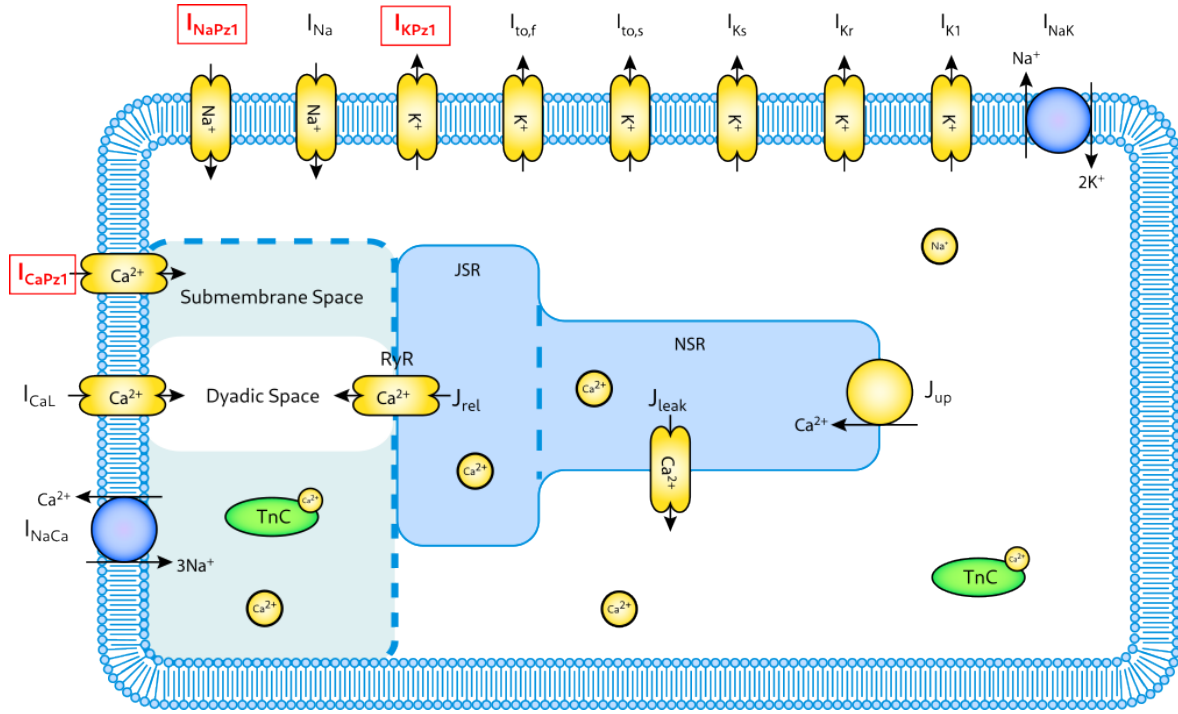


**Figure 2:** Schematic of the proposed lumped parameter cell model based on the Mahajan-Shiferaw rabbit ventricular cardiomyocyte model [41]. The new Piezo1 associated currents ( $I_{KPz1}$ ,  $I_{NaPz1}$  and  $I_{CaPz1}$ ) are highlighted inside boxes with bold-red fonts. JSR is the junctional sarcoplasmic reticulum and NSR is the non-junctional sarcoplasmic reticulum. The remaining currents and fluxes are defined as in the original model [41].

integrated the new Piezo1 model as follows under some assumptions regarding the induced currents. First, we assume that the ions do not interact with each other in the ion channel. Second, the generated current is Ohmic. This translates to the following current formulation for ions flowing through the Piezo1 channel

$$I_{Pz1} = \underbrace{p_O \bar{g}_K (\varphi_m - E_{K,s})}_{:=I_{KPz1}} + \underbrace{p_O \bar{g}_{Na} (\varphi_m - E_{Na,s})}_{:=I_{NaPz1}} + \underbrace{p_O \bar{g}_{Ca} (\varphi_m - E_{Ca,s})}_{:=I_{CaPz1}}, \quad (1)$$

where  $p_O$  is the open probability of the Piezo1 channel, given by the probability of being in the open state  $O$  of the novel Markov chain formulation shown in fig. 1. The quantities  $\bar{g}_K$ ,  $\bar{g}_{Na}$ , and  $\bar{g}_{Ca}$  are the maximal normalized conductances for the respective ion fluxes, and  $E_{K,s}$ ,  $E_{Na,s}$ ,  $E_{Ca,s}$  are the corresponding Nernst potentials (cf. [31, Ch.3.1]) related to the submembrane space ion concentrations. Since the Mahajan cell model only tracks intracellular concentrations for  $Na^+$  and assumes constant intracellular  $K^+$ , we approximate  $E_{K,s}$  and  $E_{Na,s}$  as in the original model via

$$E_{Na,s} \approx \frac{RT}{F} \ln \frac{[Na^+]_o}{[Na^+]_i}, \quad E_{K,s} \approx \frac{RT}{F} \ln \frac{[K^+]_o + pr_{NaK} [Na^+]_o}{[K^+]_i + pr_{NaK} [Na^+]_i}, \quad (2)$$

where  $pr_{NaK}$  is unknown and will be studied in the results section. The Nernst potentials for  $E_{Ca,s}$  are computed as

$$E_{Ca,s} = \frac{RT}{2F} \ln \frac{[Ca^{2+}]_o}{[Ca^{2+}]_s}. \quad (3)$$

The resulting current  $I_{Pz1}$  is added to the total transmembrane current.

In the next step we simplify the expressions for the maximal conductances by incorporating information from experiments. We first assume that the conductances of Piezo1 between species are approximately equal. Gnanasambandam et al. [23] found that, for single Piezo1 ion channels in isolation, the conductance of  $\text{Ca}^{2+}$  is  $\approx 12$  pS. In the absence of  $\text{Ca}^{2+}$ , the conductance of  $\text{Na}^+$  is about 80% the conductance of  $\text{K}^+$ . Together with the information that the reversal potential of Piezo1 is about 0 mV, we obtain a conductance of  $g_K = g_{Ca} E_{Ca,s} / (-E_{K,s} - 0.8 E_{Na,s}) \approx 52$  pS for  $\text{K}^+$ , which is close to the reported range (47 – 53 pS between  $-80$  mV and  $-100$  mV [23]). Gnanasambandam et al. [23] have also shown that the conductance of  $\text{K}^+$  is reduced by about 25% in the presence of  $\text{Ca}^{2+}$ . With the additional information that for Ohmic ion channels we have  $\bar{g}_i := N_{Pz1} g_i$ , this allows us to reduce the number of parameters, as now only the average number of Piezo1 ion channels per cell ( $N_{Pz1}$ ) is unknown. Therefore, we study the effect of  $N_{Pz1}$  in the results section as a normalized scaling parameter  $scaling := N_{Pz1} 10^{-6} / 52$ .

The new currents now change the ionic fluxes, which have to be added to the model. In the following  $J_{\square}$  denotes an ionic flux and  $I_{\square}$  the associated ionic current, as defined in eq. (1). Experimental studies suggest that Piezo1 channels are primarily located in the t-tubular membrane [30, 32]. Since we hypothesize that the influx of ions has no significant *direct* contribution to the calcium cycling within the dyadic clefts – and hence to calcium-induced calcium release (CICR) – in our model we do not link the Piezo1 channel directly to the dyadic clefts but rather to the submembrane space. In this location, the Piezo1 channel indirectly contributes to the calcium cycling via membrane depolarization and the release of calcium to the membrane subspace near the dyadic clefts, as highlighted in the schematic cell model in fig. 2. To enforce conservation of the ionic concentrations consistently with the remaining Mahajan-Shiferaw model, we have to modify the evolution equations for the submembrane calcium concentration  $[\text{Ca}^{2+}]_s$

$$d_t[\text{Ca}^{2+}]_s = \beta_s \left( \frac{v_i}{v_s} (J_{\text{rel}} - J_d + J_{\text{CaL}} + \mathbf{J_{CaPz1}} + J_{\text{NaCa}}) - J_{\text{trpn}}^s \right), \quad (4)$$

where the flux is consistently computed as  $J_{\text{CaPz1}} = -\frac{C_m}{2Fv_i} I_{\text{CaPz1}}$ , and the evolution of the intracellular sodium concentration  $[\text{Na}^+]_i$

$$d_t[\text{Na}^+]_i = \alpha' (I_{\text{Na}} + \mathbf{I_{NaPz1}} + 3I_{\text{NaCa}} + 3I_{\text{NaK}}), \quad (5)$$

to include the novel ionic flux. Note that potassium is not explicitly tracked in this model. Here  $\alpha'$  is a factor to translate the Ohmic currents to its corresponding ion flux with correct magnitude,  $\beta_s$  a binding coefficient,  $v_i$  and  $v_s$  the representative volumes of the intracellular and submembrane compartments. All values for these parameters and the formulations for the currents, fluxes, and their evolution laws, even the ones not directly presented here, are taken from the original paper [41]. A schematic of the proposed lumped parameter cell model is given in fig. 2. The modified cell model, together with scripts for all experiments, are provided in the supplementary materials. Our novel ion channel model is integrated into the Mahajan-Shiferaw via *CellML 2.0* [12] using *OpenCOR* [20].

## 2.2 Parameter Optimization

The parameters for the new Markov chain model have been obtained by formulating an optimization problem to fit some of the transmembrane potential trajectories from the experiments presented in [44] on outside-out patches of N2a cells containing wild type mouse Piezo1 channels. All simulations required for the parameter adjustment have been performed using ABDF2 [10] and *Sundials CVODE* [27] (for validation) via *DifferentialEquations.jl* [57]. These schemes provided good trade-offs between robustness and performance in the simulations. To

$c_1^e$	$c_2^m$	$c_2^e$	$c_3^e$	$c_4^m$	$c_4^e$	$c_5^e$	$c_6^e$	$c_7^e$	$c_8^e$
-0.0064121	0.124268	-0.0258118	0.0142561	0.0406628	0.0352718	0.0182107	-0.0301922	0.059666	-0.0082322
$r_1$	$r_2$	$r_3$	$r_4$	$r_5$	$r_6$	$r_7$	$r_8$		
0.00504513	0.00043889	0.00160264	0.0182634	1.99342e-6	0.0132307	9.2139e-5	0.0034847		

**Table 1:** Parameters of the Piezo1 model used in the computational studies presented in sec. 3. This table is also provided as a csv file in the supplementary materials.

find a suitable set of parameters, we have decided to minimize a normalized Huber-type Lasso loss function with normalized data:

$$L(\mathbf{p}, \bar{\mathbf{g}}) = \sum_{E \in \mathcal{E}} \sqrt{\frac{1}{|T_E|} \sum_{t_i \in T_E} H \left( P_O(t_i; \mathbf{p}) g_i \frac{\varphi_{m_E}}{\varphi_{m_{\max}}} - \bar{i}_E(t_i) \right)} + \gamma \|\mathbf{p}\|_1, \quad (6)$$

where  $H$  is the Huber function [28] with continuation at 1, i.e.  $H(x) = \min(|x|, x^2)$ ,  $\mathcal{E}$  is the set of experiments,  $T_E$  is the set of time points at which the normalized currents  $\bar{i}_E(t_i)$  are known,  $\varphi_{m_E}$  is the clamped voltage of the current experiment in mV,  $\varphi_{m_{\max}} = 80$  mV is the absolute value of the maximum clamped voltage, and  $P_O(t_i; \mathbf{p})$  is the open probability of a simulated group of Piezo1 ion channels at a specific time point  $t_i$  using the parameters  $\mathbf{p}$ . Note that, while the experiments [44, Fig. 1b] revealed that the conductivity of Piezo1 is slightly nonlinear, it can be approximated reasonably well by a constant. Furthermore, we use different bulk conductivities per experiment, denoted by  $g_i$  for experiment  $i$ , because the experiments have been conducted on different patches having different numbers of ion channels, resulting in different observed currents.

As the parameter optimization problem contains exponential functions, the chosen Huber-type loss has shown practical advantage over the classical root mean squared error (RMSE) in our experiments. Gradient information far from the optimum are naturally more limited, since the derivative of the Huber function is naturally bounded through its linear tails. The loss function (as well as other commonly used loss functions like RMSE) is not convex though. This is also partly due to the nature of the model itself, which contains parameters that appear nonlinearly in the equations. Hence, we have to deploy a global optimization procedure to obtain accurate parameters. For the optimization we utilize L-BFGS [38] with random initial guesses (N=1000). Initial parameter guesses were uniformly sampled from the interval  $[-1, 1]$  for each parameter. For the parameter optimization, we have normalized the transition functions by choosing  $p = \bar{p}/70$  and  $\Delta\mu = \Delta\bar{\mu}/140$ , such that  $p \in [0, 1]$  and  $\Delta\mu \in [-1, 1]$ .

For each numerical experiment evaluated in the loss function, we first allow the model to equilibrate by simulating 20s without mechanical stimuli (zero pressure stimulus) and a constant experiment-dependent voltage. At the beginning of each numerical experiment, we set the initial probability to be concentrated at the state  $C$ , i.e.,  $C = 1$ , and the other states are set to, i.e.,  $I_f = I_s = O = 0$ . This initialization procedure resembles the initial state of the real experimental setup. We proceed by simulating the protocols described in each experiment as shown in Figures 1a, 2a, 2c and 2f from [44]. The experimental results shown in the remaining figures were reserved for validating the calibrated model. The optimized parameter set is given in table 1, as well as in the supplementary material in a machine readable format. Our optimization studies yield that  $\gamma = 0$  leads to the best match with the experimental results, which suggests that all parameters are necessary to fit the experiments, i.e., all connections must be voltage-dependent in the proposed Markov chain model formulation.



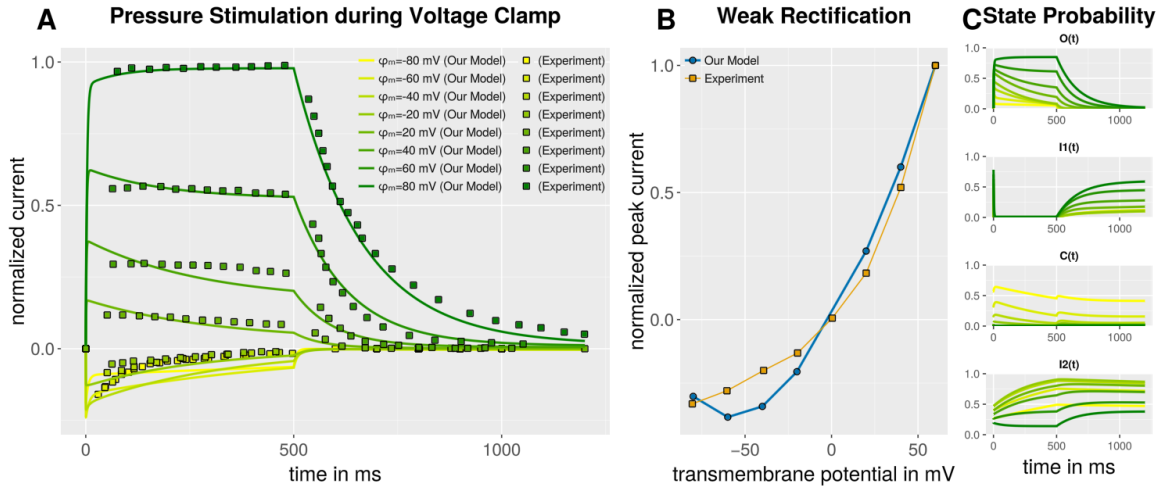


**Figure 3:** Simulation vs. experimental results from [44, Fig. 1] in the physiological regime of cardiomyocytes. **A:** Normalized currents when applying a saturating pressure stimulus (length 500 ms) during voltage clamp (see legend  $\varphi_m$ ). The predicted current traces match well the experimental results, although further quantitative improvements are possible. The monoexponential, positively voltage-dependent current decay after releasing the pressure is consistent with the observation in [64]. **B:** Normalized current amplitudes during a pressure step in voltage clamp as described in [44]. Our model also predicts qualitatively well the weak outward rectification of the ion channel. **C:** Probabilities of the specific states corresponding to the simulations in **A**.

### 3 Results

In this section we study the response of the modified Mahajan-Shiferaw cell model with integrated Piezo1 ion channel and how it can replicate published experimental results. The files necessary to reproduce all simulations are provided in the supplementary materials. In the first two studies, the Piezo1 model is initialized by setting the initial state  $C = 1$  and  $I_s = I_f = O = 0$ . The Piezo1 model is then simulated for 20 seconds using zero pressure and a constant voltage matching the voltage at the beginning of the corresponding computational experiment.

First, we investigate whether the voltage-modulated kinetics are sufficient to explain the voltage-dependent inactivation experiments shown in [44, Fig. 1] and whether the ion channel shows weak rectification in the physiological voltage range. The results of this first study are summarized in fig. 3. We observe that our proposed Markov chain captures well the voltage-dependent inactivation and predicts reasonably well the weak rectification behavior in the physiological voltage range for cardiomyocytes ( $-80$  mV to  $50$  mV). The proposed model is also able to qualitatively represent the transient response during pressure-clamp experiments at different voltages. When comparing to the data shown in [64, Fig. 1], where a different experimental setup (i.e., with regard to cell type and stimuli protocol) is considered, the proposed model still represents well the experimental observations. Specifically, the decay after releasing the pressure stimuli is well represented, at least qualitatively, by our model even when the model parameters are not adjusted to this new experimental setup.

In a second set of computational studies of the Piezo1 model, its desensitization and reversibility is investigated [44]. To carry out these studies, we have designed protocols matching the described experiments in [44, Fig. 2]. As before, we compare the current traces computed by our model with the experimentally measured counterparts. The results are illustrated in fig. 4. We can observe that key features are qualitatively well captured by our model. The model desensitizes when exposed to pressure trains at negative electrochemical driving forces.

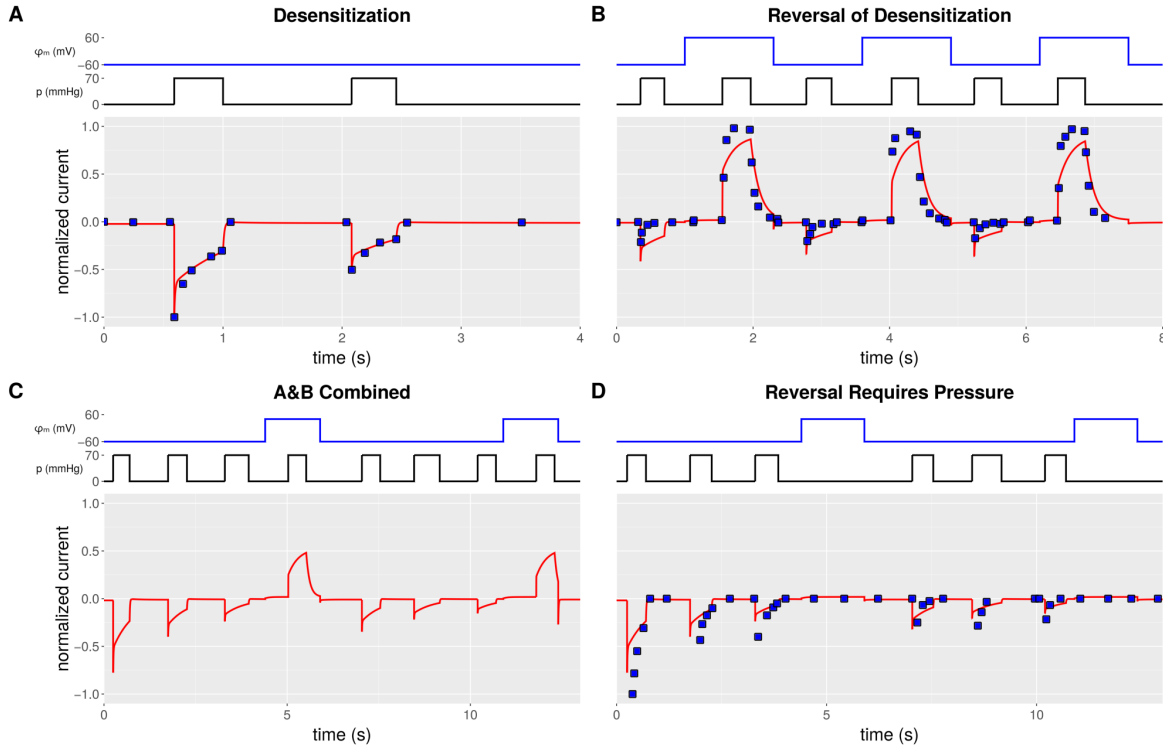


**Figure 4:** Simulation vs. experimental results from [44, Fig. 2]. Experimental data is shown using blue square markers and the corresponding numerical results are reported with a solid red line. The curves above each subfigure describe the protocol in terms of applied pressure and transmembrane potentials over time. **A:** PIEZO ion channels are known to desensitize when exposed to repeated mechanical stimulation at negative transmembrane potentials. Our model is able to reproduce this phenomenon well. **B:** As shown in [44], mechanical stimulation at positive transmembrane potential reverts desensitization. **C&D:** Reversal of desensitization requires positive electrochemical driving forces  $\Delta\mu$  and pressure acting on the membrane as shown in [44].

This desensitization is reset when a pressure step is applied at positive electrochemical driving forces. When only exposed to positive electrochemical driving forces without applying a pressure step, the model does not significantly reset, as shown in the experiments.

Finally, we study the experiments by Quinn and Kohl [55] with our modified ventricular cardiomyocyte model. We recall that, in the experiment by Quinn and Kohl [55], a Langendorff perfused rabbit heart is stimulated mechanically and electrically with different protocols. The stimuli are applied with a linear piston and an electrode, respectively. The key observations in this experiment are that: 1) mechanical capture is lost and the number of mechanical stimuli until loss of capture is inversely proportional to the stimuli frequency; and 2) loss of capture is faster (in terms of number of applied mechanical stimuli until loss of capture) when alternating mechanical and electrical stimuli are applied. In order to systematically study the free parameters  $pr_{NaK}$  and *scaling* (see sec. 2.1.3), we introduce the simplifying assumption that we can study the qualitative response of the perfused heart at a material point level. In making this simplifying assumption, we neglect all heterogeneities in cell types in the perfused heart, as well as all gradients in mechanical and electrical stimuli. We discuss the limitations introduced by this simplification in detail in section 4.1.

For our computational studies at the material point level, we approximate the experimentally applied mechanical stimuli (induced by a linear piston) as pressure steps with amplitude of 50 mmHg for 10 ms. The electrical stimulus is also modeled as a step function with an

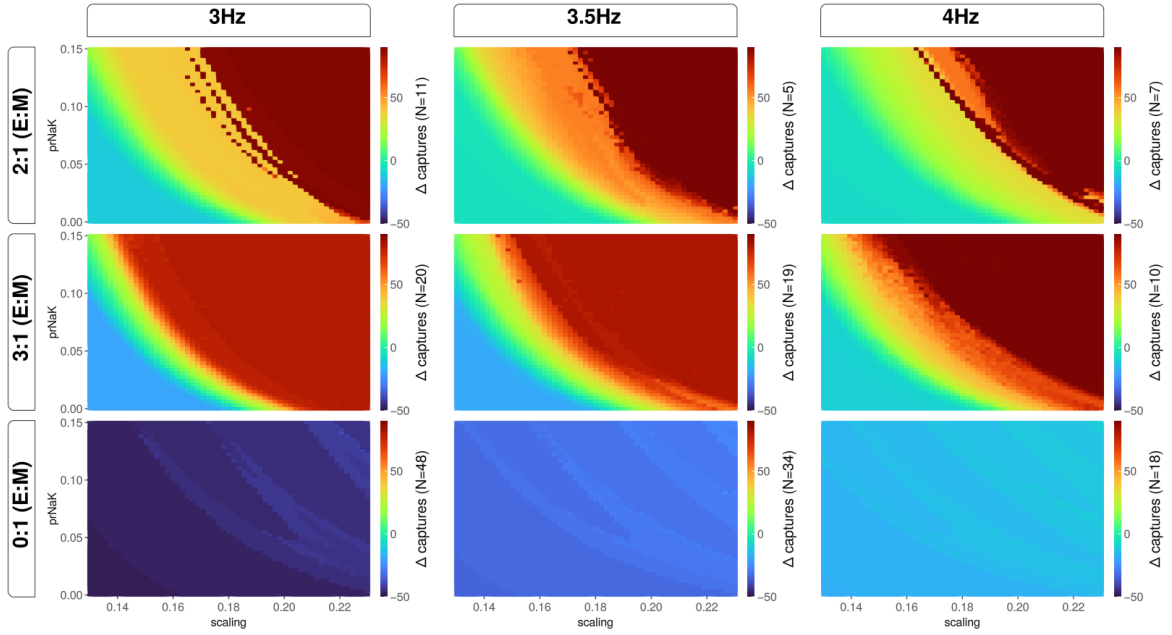


**Figure 5:** Differences in the total number of captured mechanical stimuli between the computational results and the experimental observations for different choices of  $pr_{NaK}$  and  $scaling$  parameters in the proposed model (results are reported as number of captured mechanical stimuli in the simulations minus the number of captured mechanical stimuli in the experiments – The latter is equal to the number ‘N’ reported in each subfigure). The scaling parameter corresponds to approximately 2,500 to 4,230 Piezo1 ion channels on the cell membrane. Each plot represents a different experimental protocol (rows) and a different electromechanical pacing rate (columns). In the associated colorbars  $N$  refers to the number of captured mechanical stimuli in the real experiment by Quinn and Kohl [55] used as reference. We can clearly observe a non-trivial relationship between the parameters and the number of captured mechanical stimuli in each experiment.

amplitude of 15 pA and a width of 3 ms. We explored the parameter space in two steps. First, a coarse parameter grid was utilized (not shown) to narrow down the parameters’ space to reproduce the total number of captured mechanical stimuli recorded in the experiments. In this first sweep of the parameter space, we identified that the conductance scaling parameter should be between 0.13 and 0.23, while the relative NaK contribution should be between 0.0 and 0.16. This region was then analyzed using a fine grid. The resulting difference in the total number of captured mechanical stimuli between the computational studies and experiment are presented in fig. 5 for three protocols at three different frequencies. The proposed model is able to reproduce, for some parameterizations, the experimental observation that the loss of capture in 2:1 (E:M) pacing occurs faster than in 3:1 (E:M) pacing. However, none of the studied parameter combinations can reproduce all experimental findings by [55] quantitatively. Furthermore, no simulation in the studied parameter range is able to reproduce the experimental observation that alternating mechanical and electrical stimuli lead to faster loss of mechanical capture than during mechanical pacing alone. If we describe the study above as an optimization problem with standard sum of squared errors between the computational results and the experimental observations, then the resulting loss surface is presented in fig. 6.

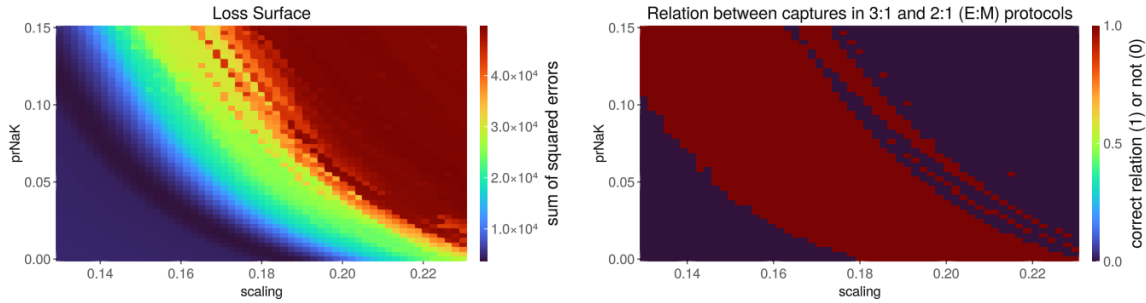


**Figure 6:** **Left:** Sum of the squared differences from fig. 5 across the different pacing protocol and frequencies showing the parameter values for  $pr_{NaK}$  and  $scaling$  corresponding to the lowest overall error (see colorbar). **Right:** In the electromechanical pacing experiments by Quinn and Kohl [55, Fig. 6] it can be observed that the number of captured mechanical stimuli in the 3:1 (E:M) protocol is larger than the number of captured mechanical stimuli in the 2:1 (E:M) protocol. All parameter combinations which represent this qualitative relation are shown as red pixels (see colorbar).

## 4 Discussion & Conclusion

We have presented an improved Piezo1 ion channel model formulated as a continuous time Markov chain and integrated it into a popular ventricular cardiomyocyte model [41]. To the best of the authors' knowledge, this is the first time that a Piezo1 channel appears as the driver for the stretch-activated current  $I_{SAC,NS}$  in a mathematical cardiomyocyte model. The proposed voltage-modulated Piezo1 formulation reproduces a wide range of experimental results from different groups, including voltage-dependent desensitization and the reversal of desensitization in the presence of positive electrochemical driving forces. Additionally, after integrating the proposed Piezo1 formulation into the cardiomyocyte model, our studies enable to qualitatively explain some of the experimental observations from Quinn and Kohl [55]. First, the loss of mechanical capture in cardiac tissues can – at least in part – be attributed to the Piezo1 channel. Second, it is likely that the voltage-modulation of the Piezo1 channel plays a major role in explaining the differences in the number of captured mechanical stimuli observed during the electromechanical pacing of cardiac tissues across pacing protocols and frequencies. However, significant quantitative differences still exist between the number of experimentally observed and numerically simulated captured mechanical stimuli. In the next section, we discuss several reasons for the observed differences and potential avenues to further improve the proposed model. In addition to improving the proposed model, further mechanisms independent of Piezo1 channels may also play an important role in explaining the experimental observations reported by Quinn and Kohl [55].

### 4.1 Limitations

It has been shown in several experiments that repeated mechanical stimuli can lead to inactivation (e.g., [13, 25, 34, 44]). Experiments of Moroni et al. [44] suggest that the inactivation can be reverted with an outward flux of ions in symmetric  $K^+$  buffers and positive transmembrane voltages. However, this setup, which we used as ground truth data to fit the ion channel model's kinetic parameters, has some limitations. Symmetric  $K^+$  buffers are not the cells' physiological environment. It is hence unclear whether the observed kinetics in [44] is directly translatable to more complex ionic environments. For example, inactivation of mouse Piezo1 channels can be observed at positive transmembrane potentials in more complex ionic environments [23, Fig. 2A]. Hence, some of the discrepancies in the number of captured stimuli simulated with our proposed cardiomyocyte model and observed in the electromechanical

spacing protocols may depend on the simplifications made (e.g., the calibration of the kinetic parameters) when integrating the Piezo1 ion channel into the Mahajan-Shiferaw cell model. Currently, sufficient quantitative experimental data is not available to develop a more precise description of electrochemical driving force of our Piezo1 ion channel model. Hence, we decided to develop this first model with a simplistic description of the before-mentioned electrochemical driving forces (cf. eq. 1).

A second problem we encountered in developing the proposed model, is the lack of publicly available experimental data specific to the rabbit Piezo1 electrophysiology kinetics. The parameters for our mathematical model have been estimated using mouse neuroblastoma (N2a) derived Piezo1 kinetics by [44]. Our model is able to describe qualitatively well all the experimental observations regarding the wildtype Piezo1 channel. However, since there are physiological differences between mouse and rabbit, as well as between neurons and cardiomyocytes, there is the possibility that the rabbit Piezo1 ion channel kinetics differs sufficiently to cause significant deviations in the modeled response. This hypothesis is supported by recent work on comparing Piezo1 ion channels in bone marrow with those in cardiomyocytes [63]. Furthermore, as already discussed in sec 2.1.1, experiments suggest that Piezo1 ion channels colocalize with TRP channels [30, 66]. The potential interaction between these ion channels will likely modify their kinetics and hence the generated ionic fluxes. It has also been demonstrated in the paper by Moroni et al. [44] that there are observable differences in Piezo1 ion channel kinetics across the different kingdoms. Additional experiments may help overcoming these limitations. In particular, studies using cardiomyocyte-derived Piezo1 patches and whole-cell experiments can help to better understand the role of Piezo1 in the observed loss of capture and other cellular processes.

Another component in our model that needs further investigation is the electrochemical driving force  $\Delta\mu$ . In our Piezo1 ion channel model, we assume that  $\Delta\mu$  is equivalent to the transmembrane voltage. We made this assumption based on experimental observations showing that the reversal potential of the Piezo1 channel is close to zero [14]. However, we also construct the transmembrane current as the sum of three independent Ohmic currents with separate driving forces (cf. eq. (1)), which are not coupled to the driving force in the Piezo1 channel. This means that the effect of the driving forces may not match with the reversal potential in the Piezo1 channel being zero. The motivation for the separation of the total Piezo1 current into the Ohmic currents is simple. Since Piezo1 generates enough current to depolarize the membrane, there has to be also significant ionic flux and hence, since the number of different ions has to be conserved in our model, we had to adjust the concentration balance equations. However, in the Mahajan-Shiferaw model, the balance equations require separate currents, and hence we decided to additively split the current as described. This represents the simplest possible formulation since potentially nonlinear or multiplicative couplings are not included. Future work should revisit this assumption when more experimental data on the transmembrane currents becomes available.

Finally, in investigating the electromechanical pacing of cardiac tissue by Quinn and Kohl [55] we have introduced the simplification of reproducing these experimental results at the material point level. In doing so, we ignored any potential influence of the heart's natural electrical pacing (e.g., pacing from the SA node). This confounds the comparison of the loss of capture in our simulations and the experiments, as the intracellular ionic concentrations of the cardiomyocyte model evolve differently than in the experiment where the natural electrical pacing is present. Second, on a structural level, the piston in the experiments generates inhomogeneous pressure gradients in the Langendorff perfused heart. Since in our setup we study single material points, this effect is a priori not captured. We do not expect that these simplifications will significantly affect the presented results from a qualitative point of

view. More significant in these simulations can be the effect of the contractile behavior of the cardiomyocytes which has been neglected in the simulated response focusing on the material point. These, however, would significantly depend on the structural response, which in turn would depend on boundary conditions associated, e.g., with the unknown pressure in the intraventricular balloon. The related changes in tissue pressure and stretch would impact the response in the Piezo1 ion channel.

## 4.2 Conclusions

We presented a mathematical model and numerical simulations that integrate mechano-electric feedback at the cellular level. This is a first step into a mechanistic understanding of emergency pacing as well as physiological pathways governing growth and remodeling processes at the cellular scale.

In particular, to understand emergency pacing procedures in detail, more studies have to be conducted at the cellular level in tandem with modelers, as these cellular models bridge the microscopic protein scale with the macroscopic tissue and organ scales. Subjects receiving an emergency pacing procedure may have underlying disease conditions leading to the cardiac arrest. Cardiac arrest can also be triggered chemically (e.g., due to substance abuse, substance intolerance or accidental exposure to cardiotoxic substances), electrically, or mechanically via blunt force, as for example in *Comotio Cordis*, leading potentially to the application of an emergency pacing procedure. Future studies on the topic of emergency pacing protocols should take these different circumstances of cardiac arrest into account when deriving hypotheses, constructing enhanced models, and setting up simulation experiments. We hope that the presented framework will provide a solid first step to develop subsequent studies in the broader context of electromechanical pacing. By sharing our baseline model in the form of CellML files, we would like to encourage other groups to use our framework to derive more refined integrations into cardiomyocytes, and potentially other cell models where Piezo1 ion channels play an important functional role.

## Acknowledgement

Financial funding by the German Research Foundation (Deutsche Forschungsgemeinschaft, DFG), project ID 544827709, is highly appreciated by the authors Balzani and Ogiermann.

## References

- [1] K. N. Aronis, R. Ali, and N. A. Trayanova. The role of personalized atrial modeling in understanding atrial fibrillation mechanisms and improving treatment. *Int. J. Cardiol.*, 287:139–147, 2019. ISSN 01675273. doi: 10.1016/j.ijcard.2019.01.096.
- [2] C. M. Augustin, M. A. F. Gsell, E. Karabelas, E. Willemen, F. W. Prinzen, J. Lumens, E. J. Vigmond, and G. Plank. A computationally efficient physiologically comprehensive 3D–0D closed-loop model of the heart and circulation. *CMAME*, 386:114092, 2021. ISSN 0045-7825. doi: 10.1016/j.cma.2021.114092.
- [3] J. Backs. Piezo1 links mechanosensation to cardiac growth. *Nat Cardiovasc Res*, 1(6): 533–534, 2022. ISSN 2731-0590. doi: 10.1038/s44161-022-00084-y.
- [4] C. Bae, R. Gnanasambandam, C. Nicolai, F. Sachs, and P. A. Gottlieb. Xerocytosis is caused by mutations that alter the kinetics of the mechanosensitive channel PIEZO1.

- Proc. Natl. Acad. Sci. U.S.A.*, 110(12), 2013. ISSN 0027-8424, 1091-6490. doi: 10.1073/pnas.1219777110.
- [5] C. Bae, P. A. Gottlieb, and F. Sachs. Human PIEZO1: Removing Inactivation. *Biophysical Journal*, 105(4):880–886, 2013. ISSN 00063495. doi: 10.1016/j.bpj.2013.07.019.
- [6] F. Bartoli, E. L. Evans, N. M. Blythe, L. Stewart, E. Chuntharpursat-Bon, M. Debant, K. E. Musialowski, L. Lichtenstein, G. Parsonage, T. S. Futers, N. A. Turner, and D. J. Beech. Global PIEZO1 Gain-of-Function Mutation Causes Cardiac Hypertrophy and Fibrosis in Mice. *Cells*, 11(7):1199, 2022. ISSN 2073-4409. doi: 10.3390/cells11071199.
- [7] S. M. Cahalan, V. Lukacs, S. S. Ranade, S. Chien, M. Bandell, and A. Patapoutian. Piezo1 links mechanical forces to red blood cell volume. *eLife*, 4:e07370, 2015. ISSN 2050-084X. doi: 10.7554/eLife.07370.
- [8] J. Camps, B. Lawson, C. Drovandi, A. Mincholé, Z. J. Wang, V. Grau, K. Burrage, and B. Rodriguez. Inference of ventricular activation properties from non-invasive electrocardiography. *arXiv:2010.15214 [eess, q-bio]*, 2020.
- [9] L. Cardone-Noott, A. Bueno-Orovio, A. Mincholé, N. Zemzemi, and B. Rodriguez. Human ventricular activation sequence and the simulation of the electrocardiographic QRS complex and its variability in healthy and intraventricular block conditions. *EP Eur.*, 18 (suppl\_4):iv4–iv15, 2016. doi: 10.1093/europace/euw346.
- [10] E. A. Celaya, J. J. A. Aguirrezabala, and P. Chatzipantelidis. Implementation of an Adaptive BDF2 Formula and Comparison with the MATLAB Ode15s. *Procedia Computer Science*, 29:1014–1026, 2014. ISSN 18770509. doi: 10.1016/j.procs.2014.05.091.
- [11] J. Chong, D. De Vecchis, A. J. Hyman, O. V. Povstyan, M. J. Ludlow, J. Shi, D. J. Beech, and A. C. Kalli. Modeling of full-length Piezo1 suggests importance of the proximal N-terminus for dome structure. *Biophysical Journal*, 120(8):1343–1356, 2021. ISSN 00063495. doi: 10.1016/j.bpj.2021.02.003.
- [12] M. Clerx, M. T. Cooling, J. Cooper, A. Garny, K. Moyle, D. P. Nickerson, P. M. F. Nielsen, and H. Sorby. CellML 2.0. *Journal of Integrative Bioinformatics*, 17(2-3): 20200021, 2020. ISSN 1613-4516. doi: 10.1515/jib-2020-0021.
- [13] B. Coste, J. Mathur, M. Schmidt, T. J. Earley, S. Ranade, M. J. Petrus, A. E. Dubin, and A. Patapoutian. Piezo1 and Piezo2 Are Essential Components of Distinct Mechanically Activated Cation Channels. *Science*, 330(6000):55–60, 2010. ISSN 0036-8075, 1095-9203. doi: 10.1126/science.1193270.
- [14] B. Coste, B. Xiao, J. S. Santos, R. Syeda, J. Grandl, K. S. Spencer, S. E. Kim, M. Schmidt, J. Mathur, A. E. Dubin, M. Montal, and A. Patapoutian. Piezo proteins are pore-forming subunits of mechanically activated channels. *Nature*, 483(7388): 176–181, 2012. ISSN 0028-0836, 1476-4687. doi: 10.1038/nature10812.
- [15] D. De Vecchis, D. J. Beech, and A. C. Kalli. Molecular dynamics simulations of Piezo1 channel opening by increases in membrane tension. *Biophysical Journal*, 120(8):1510–1521, 2021. ISSN 00063495. doi: 10.1016/j.bpj.2021.02.006.
- [16] D. Deng, H. J. Arevalo, A. Prakosa, D. J. Callans, and N. A. Trayanova. A feasibility study of arrhythmia risk prediction in patients with myocardial infarction and preserved ejection fraction. *EP Eur.*, 18(suppl\_4):iv60–iv66, 2016. ISSN 1099-5129, 1532-2092. doi: 10.1093/europace/euw351.

- 
- [17] H. Eyring. The Activated Complex in Chemical Reactions. *The Journal of Chemical Physics*, 3(2):107–115, 1935. ISSN 0021-9606, 1089-7690. doi: 10.1063/1.1749604.
- [18] Henry. Eyring. The Activated Complex and the Absolute Rate of Chemical Reactions. *Chem. Rev.*, 17(1):65–77, 1935. ISSN 0009-2665, 1520-6890. doi: 10.1021/cr60056a006.
- [19] M. Fedele, R. Piersanti, F. Regazzoni, M. Salvador, P. C. Africa, M. Bucelli, A. Zingaro, L. Dede', and A. Quarteroni. A comprehensive and biophysically detailed computational model of the whole human heart electromechanics. *Computer Methods in Applied Mechanics and Engineering*, 410:115983, 2023. ISSN 00457825. doi: 10.1016/j.cma.2023.115983.
- [20] A. Garny and P. J. Hunter. OpenCOR: A modular and interoperable approach to computational biology. *Frontiers in Physiology*, 6:26, 2015. ISSN 1664-042X. doi: 10.3389/fphys.2015.00026.
- [21] T. Gerach, S. Schuler, J. Fröhlich, L. Lindner, E. Kovacheva, R. Moss, E. M. Wülfers, G. Seemann, C. Wieners, and A. Loewe. Electro-Mechanical Whole-Heart Digital Twins: A Fully Coupled Multi-Physics Approach. *Mathematics*, 9(11):1247, 2021. doi: 10.3390/math9111247.
- [22] A. Gerbi, L. Dedè, A. Quarteroni, A. Gerbi, L. Dedè, and A. Quarteroni. A monolithic algorithm for the simulation of cardiac electromechanics in the human left ventricle. *Mathematics in Engineering*, 1(1):1–37, 2019. ISSN 2640-3501. doi: 10.3934/Mine.2018.1.1.
- [23] R. Gnanasambandam, C. Bae, P. A. Gottlieb, and F. Sachs. Ionic Selectivity and Permeation Properties of Human PIEZO1 Channels. *PLoS ONE*, 10(5):e0125503, 2015. ISSN 1932-6203. doi: 10.1371/journal.pone.0125503.
- [24] S. Göktepe, A. Menzel, and E. Kuhl. The generalized Hill model: A kinematic approach towards active muscle contraction. *Journal of the Mechanics and Physics of Solids*, 72: 20–39, 2014. ISSN 0022-5096. doi: 10.1016/J.JMPS.2014.07.015.
- [25] P. A. Gottlieb, C. Bae, and F. Sachs. Gating the mechanical channel Piezo1: A comparison between whole-cell and patch recording. *Channels*, 6(4):282–289, 2012. ISSN 1933-6950, 1933-6969. doi: 10.4161/chan.21064.
- [26] E. Grandi, D. Dobrev, and J. Heijman. Computational modeling: What does it tell us about atrial fibrillation therapy? *Int. J. Cardiol.*, 287:155–161, 2019. ISSN 01675273. doi: 10.1016/j.ijcard.2019.01.077.
- [27] A. C. Hindmarsh, P. N. Brown, K. E. Grant, S. L. Lee, R. Serban, D. E. Shumaker, and C. S. Woodward. SUNDIALS: Suite of nonlinear and differential/algebraic equation solvers. *ACM Trans. Math. Softw.*, 31(3):363–396, 2005. ISSN 0098-3500, 1557-7295. doi: 10.1145/1089014.1089020.
- [28] P. J. Huber. Robust Estimation of a Location Parameter. *Ann. Math. Statist.*, 35(1): 73–101, 1964. ISSN 0003-4851. doi: 10.1214/aoms/1177703732.
- [29] L. T. Izu, P. Kohl, P. A. Boyden, M. Miura, T. Banyasz, N. Chiamvimonvat, N. Trayanova, D. M. Bers, and Y. Chen-Izu. Mechano-electric and mechano-chemo-transduction in cardiomyocytes. *The Journal of Physiology*, 598(7):1285–1305, 2020. ISSN 1469-7793. doi: 10.1113/JP276494.



- [30] F. Jiang, K. Yin, K. Wu, M. Zhang, S. Wang, H. Cheng, Z. Zhou, and B. Xiao. The mechanosensitive Piezo1 channel mediates heart mechano-chemo transduction. *Nat Commun*, 12(1):869, 2021. ISSN 2041-1723. doi: 10.1038/s41467-021-21178-4.
- [31] J. Keener and J. Sneyd, editors. *Mathematical Physiology I: Cellular Physiology, II: Systems Physiology*. 2009.
- [32] B. Kloth, G. Mearini, F. Weinberger, J. Stenzig, B. Geertz, J. Starbatty, D. Lindner, U. Schumacher, H. Reichenspurner, T. Eschenhagen, and M. N. Hirt. Piezo2 is not an indispensable mechanosensor in murine cardiomyocytes. *Sci Rep*, 12(1):8193, 2022. ISSN 2045-2322. doi: 10.1038/s41598-022-12085-9.
- [33] A. H. Lewis and J. Grandl. Piezo1 ion channels inherently function as independent mechanotransducers. *eLife*, 10:e70988, 2021. ISSN 2050-084X. doi: 10.7554/eLife.70988.
- [34] A. H. Lewis, A. F. Cui, M. F. McDonald, and J. Grandl. Transduction of Repetitive Mechanical Stimuli by Piezo1 and Piezo2 Ion Channels. *Cell Reports*, 19(12):2572–2585, 2017. ISSN 22111247. doi: 10.1016/j.celrep.2017.05.079.
- [35] J. Li, B. Hou, S. Tumova, K. Muraki, A. Bruns, M. J. Ludlow, A. Sedo, A. J. Hyman, L. McKeown, R. S. Young, N. Y. Yuldasheva, Y. Majeed, L. A. Wilson, B. Rode, M. A. Bailey, H. R. Kim, Z. Fu, D. A. L. Carter, J. Bilton, H. Imrie, P. Ajuh, T. N. Dear, R. M. Cubbon, M. T. Kearney, K. R. Prasad, P. C. Evans, J. F. X. Ainscough, and D. J. Beech. Piezo1 integration of vascular architecture with physiological force. *Nature*, 515(7526):279–282, 2014. ISSN 0028-0836, 1476-4687. doi: 10.1038/nature13701.
- [36] J. Liang, B. Huang, G. Yuan, Y. Chen, F. Liang, H. Zeng, S. Zheng, L. Cao, D. Geng, and S. Zhou. Stretch-activated channel Piezo1 is up-regulated in failure heart and cardiomyocyte stimulated by AngII. *Am J Transl Res*, 9(6):2945–2955, 2017. ISSN 1943-8141.
- [37] G. B. Lim. Piezo1 senses pressure overload and initiates cardiac hypertrophy. *Nat Rev Cardiol*, 19(8):503–503, 2022. ISSN 1759-5002, 1759-5010. doi: 10.1038/s41569-022-00746-1.
- [38] D. C. Liu and J. Nocedal. On the limited memory BFGS method for large scale optimization. *Mathematical Programming*, 45(1-3):503–528, 1989. ISSN 0025-5610, 1436-4646. doi: 10.1007/BF01589116.
- [39] T. E. Loman, Y. Ma, V. Ilin, S. Gowda, N. Korsbo, N. Yewale, C. Rackauckas, and S. A. Isaacson. Catalyst: Fast Biochemical Modeling with Julia. Preprint, Systems Biology, 2022.
- [40] Y. Ma, S. Gowda, R. Anantharaman, C. Laughman, V. Shah, and C. Rackauckas. ModelingToolkit: A Composable Graph Transformation System For Equation-Based Modeling, 2021.
- [41] A. Mahajan, Y. Shiferaw, D. Sato, A. Baher, R. Olcese, L.-H. Xie, M.-J. Yang, P.-S. Chen, J. G. Restrepo, A. Karma, A. Garfinkel, Z. Qu, and J. N. Weiss. A Rabbit Ventricular Action Potential Model Replicating Cardiac Dynamics at Rapid Heart Rates. *Biophysical Journal*, 94(2):392–410, 2008. ISSN 0006-3495. doi: 10.1529/BIOPHYSJ.106.98160.
- [42] M. Maillet, J. H. van Berlo, and J. D. Molkenin. Molecular basis of physiological heart growth: Fundamental concepts and new players. *Nat Rev Mol Cell Biol*, 14(1):38–48, 2013. ISSN 1471-0072, 1471-0080. doi: 10.1038/nrm3495.

- [43] M. J. McMillin, A. E. Beck, J. X. Chong, K. M. Shively, K. J. Buckingham, H. I. Gildersleeve, M. I. Aracena, A. S. Aylsworth, P. Bitoun, J. C. Carey, C. L. Clericuzio, Y. J. Crow, C. J. Curry, K. Devriendt, D. B. Everman, A. Fryer, K. Gibson, M. L. Giovannucci Uzielli, J. M. Graham, J. G. Hall, J. T. Hecht, R. A. Heidenreich, J. A. Hurst, S. Irani, I. P. Krapels, J. G. Leroy, D. Mowat, G. T. Plant, S. P. Robertson, E. K. Schorry, R. H. Scott, L. H. Seaver, E. Sherr, M. Splitt, H. Stewart, C. Stumpel, S. G. Temel, D. D. Weaver, M. Whiteford, M. S. Williams, H. K. Tabor, J. D. Smith, J. Shendure, D. A. Nickerson, and M. J. Bamshad. Mutations in PIEZO2 Cause Gordon Syndrome, Marden-Walker Syndrome, and Distal Arthrogyriposis Type 5. *The American Journal of Human Genetics*, 94(5):734–744, 2014. ISSN 00029297. doi: 10.1016/j.ajhg.2014.03.015.
- [44] M. Moroni, M. R. Servin-Vences, R. Fleischer, O. Sánchez-Carranza, and G. R. Lewin. Voltage gating of mechanosensitive PIEZO channels. *Nat Commun*, 9(1):1096, 2018. ISSN 2041-1723. doi: 10.1038/s41467-018-03502-7.
- [45] R. Moss, E. M. Wülfers, R. Lewetag, T. Hornyik, S. Perez-Feliz, T. Strohbach, M. Menza, A. Krafft, K. E. Odening, and G. Seemann. A computational model of rabbit geometry and ECG: Optimizing ventricular activation sequence and APD distribution. *PLoS ONE*, 17(6):e0270559, 2022. ISSN 1932-6203. doi: 10.1371/journal.pone.0270559.
- [46] Y. A. Nikolaev, C. D. Cox, P. Ridone, P. R. Rohde, J. F. Cordero-Morales, V. Vásquez, D. R. Laver, and B. Martinac. Mammalian TRP ion channels are insensitive to membrane stretch. *Journal of Cell Science*, page jcs.238360, 2019. ISSN 1477-9137, 0021-9533. doi: 10.1242/jcs.238360.
- [47] D. Ogiermann, D. Balzani, and L. E. Perotti. The Effect of Modeling Assumptions on the ECG in Monodomain and Bidomain Simulations. In D. B. Ennis, L. E. Perotti, and V. Y. Wang, editors, *Functional Imaging and Modeling of the Heart*, volume 12738, pages 503–514. Springer International Publishing, Cham, 2021. ISBN 978-3-030-78709-7 978-3-030-78710-3. doi: \$10.1007/978-3-030-78710-3\_48\$.
- [48] D. Ogiermann, D. Balzani, and L. E. Perotti. An extended generalized hill model for cardiac tissue: Comparison with different approaches based on experimental data. In *Functional Imaging and Modeling of the Heart*, pages 555–564, Cham, 2023. Springer Nature Switzerland. ISBN 978-3-031-35302-4.
- [49] T. M. Olasveengen, M. E. Mancini, G. D. Perkins, S. Avis, S. Brooks, M. Castrén, S. P. Chung, J. Considine, K. Couper, R. Escalante, T. Hatanaka, K. K. Hung, P. Kundenchuk, S. H. Lim, C. Nishiyama, G. Ristagno, F. Semeraro, C. M. Smith, M. A. Smyth, C. Vaillancourt, J. P. Nolan, M. F. Hazinski, P. T. Morley, H. Svavarsdóttir, V. Raffay, A. Kuzovlev, J.-T. Grasner, R. Dee, M. Smith, and K. Rajendran. Adult Basic Life Support: 2020 International Consensus on Cardiopulmonary Resuscitation and Emergency Cardiovascular Care Science With Treatment Recommendations. *Circulation*, 142(16\_suppl\_1), 2020. ISSN 0009-7322, 1524-4539. doi: 10.1161/CIR.0000000000000892.
- [50] E. Passini, O. J. Britton, H. R. Lu, J. Rohrbacher, A. N. Hermans, D. J. Gallacher, R. J. Greig, A. Bueno-Orovio, and B. Rodriguez. Human in silico drug trials demonstrate higher accuracy than animal models in predicting clinical pro-arrhythmic cardiotoxicity. *Front. Physiol.*, 8(SEP), 2017. ISSN 1664042X. doi: 10.3389/fphys.2017.00668.
- [51] J. E. Pennington, J. Taylor, and B. Lown. Chest Thump for Reverting Ventricular Tachycardia. *N Engl J Med*, 283(22):1192–1195, 1970. ISSN 0028-4793, 1533-4406. doi: 10.1056/NEJM197011262832204.

- [52] G. D. Perkins, J.-T. Gräsner, F. Semeraro, T. Olasveengen, J. Soar, C. Lott, P. Van De Voorde, J. Madar, D. Zideman, S. Mentzelopoulos, L. Bossaert, R. Greif, K. Monsieurs, H. Svavarsdóttir, J. P. Nolan, S. Ainsworth, S. Akin, A. Alfonzo, J. Andres, S. Attard Montalto, A. Barelli, M. Baubin, W. Behringer, B. Bein, D. Biarent, R. Bingham, M. Blom, A. Boccuzzi, V. Borra, L. Bossaert, B. Böttiger, J. Breckwoldt, O. Brissaud, R. Burkart, A. Cariou, P. Carli, F. Carmona, P. Cassan, M. Castren, T. Christophides, C. Cimpoesu, C. Clarens, P. Conaghan, K. Couper, T. Cronberg, E. De Buck, N. De Lucas, A. De Roovere, C. Deakin, J. Delchef, B. Dirks, J. Djakow, T. Djarv, P. Druwe, G. Eldin, H. Ersdal, H. Friberg, C. Genbrugge, M. Georgiou, E. Goemans, V. Gonzalez-Salvado, P. Gradisek, J. Graesner, R. Greif, A. Handley, C. Hassager, K. Haywood, J. Heltne, D. Hendrickx, J. Herlitz, J. Hinkelbein, F. Hoffmann, S. Hunyadi Anticevic, G. Johannesdottir, G. Khalifa, B. Klaassen, J. Koppl, U. Kreimeier, A. Kuzovlev, T. Lauritsen, G. Lilja, F. Lippert, A. Lockey, C. Lott, I. Lulic, M. Maas, I. Maconochie, J. Madar, A. Martinez-Mejias, S. Masterson, S. Mentzelopoulos, D. Meyran, K. Monsieurs, C. Morley, V. Moulart, N. Mpotos, N. Nikolaou, J. Nolan, T. Olasveengen, E. Oliver, P. Paal, T. Pellis, G. Perkins, L. Pflanzl-Knizacek, K. Pitches, K. Poole, V. Raffay, W. Renier, G. Ristagno, C. Roehr, F. Rosell-Ortiz, M. Rudiger, A. Safri, L. Sanchez Santos, C. Sandroni, F. Sari, A. Scapigliati, S. Schilder, J. Schlieber, S. Schnaubelt, F. Semeraro, S. Shammet, E. Singletary, C. Skare, M. Skrifvars, M. Smyth, J. Soar, H. Svavarsdottir, T. Szczapa, F. Taccone, M. Tageldin Mustafa, A. Te Pas, K. Thies, I. Tjelmeland, D. Trevisanuto, A. Truhlar, G. Trummer, N. Turner, B. Urlesberger, J. Vaahersalo, P. Van De Voorde, H. Van Grootven, D. Wilkinson, J. Wnent, J. Wyllie, J. Yeung, and D. Zideman. European Resuscitation Council Guidelines 2021: Executive summary. *Resuscitation*, 161:1–60, 2021. ISSN 03009572. doi: 10.1016/j.resuscitation.2021.02.003.
- [53] L. E. Perotti, S. Krishnamoorthi, N. P. Borgstrom, D. B. Ennis, and W. S. Klug. Regional segmentation of ventricular models to achieve repolarization dispersion in cardiac electrophysiology modeling. *Int J Numer Method Biomed Eng*, 31(8), 2015. ISSN 2040-7947. doi: 10.1002/cnm.2718.
- [54] A. V. S. Ponnaluri, L. E. Perotti, M. Liu, Z. Qu, J. N. Weiss, D. B. Ennis, W. S. Klug, and A. Garfinkel. Electrophysiology of Heart Failure Using a Rabbit Model: From the Failing Myocyte to Ventricular Fibrillation. *PLOS Computational Biology*, 12(6):e1004968, 2016. ISSN 1553-7358. doi: 10.1371/journal.pcbi.1004968.
- [55] T. A. Quinn and P. Kohl. Comparing maximum rate and sustainability of pacing by mechanical vs. electrical stimulation in the Langendorff-perfused rabbit heart. *EP Eur.*, 18 (suppl\_4):iv85–iv93, 2016. ISSN 1099-5129, 1532-2092. doi: 10.1093/europace/euw354.
- [56] T. A. Quinn, H. Jin, P. Lee, and P. Kohl. Mechanically Induced Ectopy via Stretch-Activated Cation-Nonselective Channels Is Caused by Local Tissue Deformation and Results in Ventricular Fibrillation if Triggered on the Repolarization Wave Edge (Commotio Cordis). *Circulation: Arrhythmia and Electrophysiology*, 10(8):e004777, 2017. doi: 10.1161/CIRCEP.116.004777.
- [57] C. Rackauckas and Q. Nie. DifferentialEquations.jl – A Performant and Feature-Rich Ecosystem for Solving Differential Equations in Julia. *JORS*, 5(1):15, 2017. ISSN 2049-9647. doi: 10.5334/jors.151.
- [58] S. S. Ranade, Z. Qiu, S.-H. Woo, S. S. Hur, S. E. Murthy, S. M. Cahalan, J. Xu, J. Mathur, M. Bandell, B. Coste, Y.-S. J. Li, S. Chien, and A. Patapoutian. Piezo1, a mechanically activated ion channel, is required for vascular development in mice. *Proc. Natl. Acad.*

- Sci. U.S.A.*, 111(28):10347–10352, 2014. ISSN 0027-8424, 1091-6490. doi: 10.1073/pnas.1409233111.
- [59] A. Reed, P. Kohl, and R. Peyronnet. Molecular candidates for cardiac stretch-activated ion channels. *Glob Cardiol Sci Pract*, 2014(2):9–25, 2014. ISSN 2305-7823. doi: 10.5339/gcsp.2014.19.
- [60] C. Sánchez, G. D’Ambrosio, F. Maffessanti, E. G. Caiani, F. W. Prinzen, R. Krause, A. Auricchio, and M. Potse. Sensitivity analysis of ventricular activation and electrocardiogram in tailored models of heart-failure patients. *Med Biol Eng Comput*, 56(3):491–504, 2018. doi: 10.1007/s11517-017-1696-9.
- [61] K. Saotome, S. E. Murthy, J. M. Kefauver, T. Whitwam, A. Patapoutian, and A. B. Ward. Structure of the mechanically activated ion channel Piezo1. *Nature*, 554(7693):481–486, 2018. ISSN 0028-0836, 1476-4687. doi: 10.1038/nature25453.
- [62] E. F. Schott. On ventricular standstill [Stokes-Adams attacks] and other arrhythmias of temporary nature. *Dt Arch klin Med*, page 211, 1920.
- [63] A. Simon-Chica, A. Klesen, R. Emig, A. Chan, J. Greiner, D. Grün, A. Lothar, I. Hilgendorf, E. A. Rog-Zielinska, U. Ravens, P. Kohl, F. Schneider-Warme, and R. Peyronnet. Piezo1 stretch-activated channel activity differs between murine bone marrow-derived and cardiac tissue-resident macrophages. *The Journal of Physiology*, 602(18):4437–4456, 2024. ISSN 0022-3751, 1469-7793. doi: 10.1113/JP284805.
- [64] J. Wu, M. Young, A. H. Lewis, A. N. Martfeld, B. Kalmeta, and J. Grandl. Inactivation of Mechanically Activated Piezo1 Ion Channels Is Determined by the C-Terminal Extracellular Domain and the Inner Pore Helix. *Cell Reports*, 21(9):2357–2366, 2017. ISSN 22111247. doi: 10.1016/j.celrep.2017.10.120.
- [65] Z.-Y. Yu, H. Gong, S. Kesteven, Y. Guo, J. Wu, J. Li, S. Iismaa, X. Kaidonis, R. M. Graham, C. D. Cox, M. P. Feneley, and B. Martinac. Piezo1 and TRPM4 work in tandem to initiate cardiac hypertrophic signalling in response to pressure overload. *Biophysical Journal*, 121(3):493a, 2022. ISSN 00063495. doi: 10.1016/j.bpj.2021.11.321.
- [66] Z.-Y. Yu, H. Gong, S. Kesteven, Y. Guo, J. Wu, J. V. Li, D. Cheng, Z. Zhou, S. E. Iismaa, X. Kaidonis, R. M. Graham, C. D. Cox, M. P. Feneley, and B. Martinac. Piezo1 is the cardiac mechanosensor that initiates the cardiomyocyte hypertrophic response to pressure overload in adult mice. *Nat Cardiovasc Res*, 1(6):577–591, 2022. ISSN 2731-0590. doi: 10.1038/s44161-022-00082-0.
- [67] Z. Yue, J. Xie, A. S. Yu, J. Stock, J. Du, and L. Yue. Role of TRP channels in the cardiovascular system. *American Journal of Physiology-Heart and Circulatory Physiology*, 308(3):H157–H182, 2015. ISSN 0363-6135, 1522-1539. doi: 10.1152/ajpheart.00457.2014.
- [68] R. Zarychanski, V. P. Schulz, B. L. Houston, Y. Maksimova, D. S. Houston, B. Smith, J. Rinehart, and P. G. Gallagher. Mutations in the mechanotransduction protein PIEZO1 are associated with hereditary xerocytosis. *Blood*, 120(9):1908–1915, 2012. ISSN 0006-4971, 1528-0020. doi: 10.1182/blood-2012-04-422253.
- [69] T. Zhang, S. Chi, F. Jiang, Q. Zhao, and B. Xiao. A protein interaction mechanism for suppressing the mechanosensitive Piezo channels. *Nat Commun*, 8(1):1797, 2017. ISSN 2041-1723. doi: 10.1038/s41467-017-01712-z.

- [70] Y. Zhang and Q. Zou. A Novel Triple-gate Model for Mechanosensitive Ion Channel Piezo1. In *2022 10th International Conference on Bioinformatics and Computational Biology (ICBCB)*, pages 135–141, Hangzhou, China, 2022. IEEE. ISBN 978-1-66540-108-1. doi: 10.1109/ICBCB55259.2022.9802499.
- [71] Y. Zhang, S.-a. Su, W. Li, Y. Ma, J. Shen, Y. Wang, Y. Shen, J. Chen, Y. Ji, Y. Xie, H. Ma, and M. Xiang. Piezo1-Mediated Mechanotransduction Promotes Cardiac Hypertrophy by Impairing Calcium Homeostasis to Activate Calpain/Calcineurin Signaling. *Hypertension*, 78(3):647–660, 2021. ISSN 0194-911X, 1524-4563. doi: 10.1161/HYPERTENSIONAHA.121.17177.
- [72] W. Zheng and F. Sachs. Investigating the structural dynamics of the PIEZO1 channel activation and inactivation by coarse-grained modeling. *Proteins*, 85(12):2198–2208, 2017. ISSN 0887-3585, 1097-0134. doi: 10.1002/prot.25384.
- [73] W. Zheng, E. O. Gracheva, and S. N. Bagriantsev. A hydrophobic gate in the inner pore helix is the major determinant of inactivation in mechanosensitive Piezo channels. *eLife*, 8:e44003, 2019. ISSN 2050-084X. doi: 10.7554/eLife.44003.